Partially Uncleaved Alphavirus Replicase Forms Spherule Structures in the Presence and Absence of RNA Template

Hellström, Kirsi

2017-09

Hellström , K , Kallio , K , Utt , A , Quirin , T , Jokitalo , E , Merits , A & Ahola , T 2017 , ' Partially Uncleaved Alphavirus Replicase Forms Spherule Structures in the Presence and Absence of RNA Template ' , Journal of Virology , vol. 91 , no. 18 , e00787-17 . https://doi.org/10.1128/JVI.00787-17

http://hdl.handle.net/10138/224258
https://doi.org/10.1128/JVI.00787-17

acceptedVersion

Partially uncleaved alphavirus replicase forms spherule structures in the presence and absence of RNA template

Kirsi Hellström[1]*, Katri Kallio[1]*, Age Utt[3], Tania Quirin[1], Eija Jokitalo[2], Andres Merits[3] and Tero Ahola[1]#

[1]Department of Food and Environmental Sciences and [2]Institute of Biotechnology, University of Helsinki, Helsinki, Finland [3]Institute of Technology, University of Tartu, Tartu, Estonia

*with equal contribution

#Address correspondence to Tero Ahola, tero.ahola@helsinki.fi

Running title: Spherule formation by alphavirus replicase proteins

Keywords: replication complex, membrane, polyprotein processing, Semliki Forest virus, Sindbis virus

Abstract

Alphaviruses are positive-strand RNA viruses expressing their replicase as a polyprotein P1234, which is cleaved to four final products, nonstructural proteins nsP1-nsP4. The replicase proteins together with viral RNA and host factors form membrane invaginations termed spherules, which act as the replication complexes producing progeny RNAs. We have previously shown that the wild type alphavirus replicase requires a functional RNA template and active polymerase to generate spherule structures. However, we now find that specific partially processed forms of the replicase proteins alone can give rise to membrane invaginations, in the absence of RNA or replication. The minimal requirement for spherule formation was the expression of properly cleaved nsP4, together with either uncleaved P123, or with the combination of nsP1 and uncleaved P23. These inactive spherules were morphologically less regular compared to replication-induced spherules. In the presence of template, nsP1 + uncleaved P23 + nsP4 could efficiently assemble active replication spherules producing both negative-sense and positive-sense RNA strands. P23 alone did not have membrane affinity, but could be recruited to membranes sites in the presence of nsP1 and nsP4. These results define the set of viral components required for alphavirus replication complex assembly and suggest the possibility that it could be reconstituted from separately expressed nonstructural proteins.

Importance

All positive-strand RNA viruses extensively modify host cell membranes to serve as efficient platforms for viral RNA replication. Alphaviruses and several other groups induce protective membrane invaginations (spherules) as their genome factories. Most positive-strand viruses

produce their replicase as a polyprotein precursor, which is further processed through precise and regulated cleavages. We show here that specific cleavage intermediates of the alphavirus replicase can give rise to spherule structures in the absence of viral RNA. In the presence of template RNA, the same intermediates yield active replication complexes. Thus, partially cleaved replicase proteins play key roles that connect replication complex assembly, membrane deformation and the different stages of RNA synthesis.

Introduction

Alphaviruses are positive-strand RNA viruses belonging to the family *Togaviridae* together with rubella virus, the only member of genus *Rubivirus*. Some New World alphaviruses (e.g. Venezuelan equine encephalitis virus) can cause serious nervous system infections, whereas several Old World alphaviruses are associated with fever, rash and arthritis (1). The latter include chikungunya virus, now found throughout the world in tropical and sub-tropical regions, as well as Sindbis virus (SINV) and Ross River virus.

After entering the cell, alphaviruses induce numerous bulb-shaped membrane invagination or spherules, which are the viral replication complexes (2, 3). It is thought that progeny RNAs are released through the constricted 'neck' of the spherule, which provides a connection between the spherule interior and the cytoplasm. The alphavirus spherules are located at the plasma membrane or at endo- and lysosomal membranes (4). Flaviviruses and nodaviruses also generate replication spherules located at different membrane sites, as do many plant viruses, among which the spherule formation of bromo- and tombusviruses has been especially well characterized. Other positive-strand RNA viruses (picornaviruses, coronaviruses and hepatitis C

46 virus) induce more complex membrane alterations, including double-membrane vesicles and
47 membranous webs (5). Remarkably, membrane-associated replication is common to all positive-
48 strand RNA viruses of eukaryotes; host cell membranes are used both to provide efficient
49 platforms for RNA synthesis as well as to protect viral RNAs from cellular antiviral surveillance (6,
50 7). While the morphologies of the replication membranes have been described in detail for several
51 viruses (8, 9), the mechanisms of membrane modification and the necessary viral and cellular
52 components are still poorly understood.

53 The alphavirus genome is translated to yield polyprotein P1234, which is the
54 precursor of viral nonstructural proteins nsP1-nsP4. All four nsPs are required for RNA synthesis
55 (10-12), and they all are found at replication spherules (2, 3). The processing of P1234 takes place
56 in a defined sequence of steps, and it has been firmly established that the different processing
57 intermediates play a critical role in the strand-specificity of the replication complex. When nsP1, 2
58 and 3 are still unprocessed as P123 polyprotein, but the core polymerase subunit nsP4 is cleaved,
59 the replication complex is mainly dedicated to negative strand synthesis (12, 13). The following
60 cleavage separates nsP1 from P23, leading to the switch to predominantly positive-strand
61 synthesis in an irreversible manner. The final cleavage between nsP2 and nsP3 further enhances
62 subgenomic RNA synthesis (12).

63 We have analyzed the formation of Semliki Forest virus (SFV) spherules by using an
64 efficient *trans*-replication system, in which the replication proteins and a template RNA are
65 expressed starting from separate DNA plasmids, facilitating the dissection of molecular functions
66 (14). We have previously observed spherules only when active RNA replication is ongoing, in the
67 presence of both a functional RNA template and an enzymatically active polymerase complex (14-
68 16). However, we now find that when specific cleavage sites of the replicase are blocked, partially

processed replicase alone can generate spherule structures. By expressing protein combinations, we define the set of viral proteins required for replication complex assembly.

Results

Expression and activity of partially cleaved SFV replicases. We have previously shown that wild type SFV replicase can only form spherule structures in the presence of a replication-competent RNA template and active polymerase, and therefore we proposed that alphavirus RNA synthesis and spherule formation take place concomitantly (14-16). A mutant replicase, in which the cleavages between nsP1 and nsP2, as well as between nsP2 and nsP3 were prevented, termed P1^2^34, was capable of efficient minus strand synthesis and spherule formation (16). Subsequently, as a further control, we mutated the polymerase active site motif Gly-Asp-Asp (GDD) to Gly-Ala-Ala or GAA (the mutant is denoted nsP4^{GAA}) in the context of the latter replicase. To our surprise, we reproducibly found that the replication-incompetent polyprotein P1^2^34^{GAA} was capable of spherule formation both in the absence and presence of a template (see below for illustrations). To investigate this issue and clarify the requirements for spherule formation, we generated a larger set of partially cleavage-defective replicase constructs, in which the cleavage sites have been destroyed (denoted by ^ at the destroyed site), or the nsP2 protease has been inactivated by mutating the active site cysteine to alanine (denoted 2^{CA}) (Fig. 1A). In some of the set-ups, the replicase is provided as multiple fragments from separate plasmids. Others and we have previously shown that nsP4 can be efficiently provided *in trans* with respect to P123, when the correct N-terminus of nsP4 is ensured by using a ubiquitin-nsP4 (ubi4) fusion (12, 14). In the current experiments we also provided polyproteins starting with nsP2 as ubiquitin fusions, since the correct N-terminus of nsP2 is important for at least some of its protease activities (17). In the

92 replicase, we included enhanced green fluorescent protein (eGFP; denoted as G in polyproteins)
93 fused to nsP3 for detection of transfected cells in correlative light and electron microscopy (CLEM)
94 experiments (18). Marker gene fusions to nsP3 have been extensively used and there is no
95 evidence that they would grossly alter replicase behavior (4, 19).

96 Upon transfection, the replicases were detected by Western blotting, and their
97 activity was assessed by *Renilla* luciferase read-out (luciferase is expressed from the template
98 construct; Fig. 1A), as well as Northern blotting (Fig. 1, B-D). P123G4 and P123G+4 (ubi4 produced
99 from a separate plasmid) acted as positive controls, with efficient replicase processing, as well as
100 high luciferase activity and RNA replication (Fig. 1, B-D, lanes 3 and 4). $P12^{CA}3G4$, a totally
101 uncleaved polyprotein, could not be detected in Western blotting, probably due to its high
102 molecular mass (calculated at 297 kDa), but the protein was expressed as evidence by
103 immunofluorescence staining with antibodies against the nsPs and by eGFP autofluorescence
104 utilized in CLEM experiments (see below). There was no evidence for luciferase activity or
105 replication, in accordance with a large body of previous work showing that the cleavage of nsP4 is
106 essential for RNA synthesis and virus replication (10, 13). P1^2^3G4 and $P12^{CA}3G+4$ should be
107 equivalent, and indeed both gave rise to uncleaved P123G, as well as efficient minus strand
108 synthesis (Fig. 1, B-D, lanes 6 and 7). Since plus strand synthesis was relatively weak (small
109 increase compared to template only control), the luciferase levels were intermediate between
110 wild type replicase and negative controls.

111 Interestingly, P12^3G4, which gave rise to P23G in Western blotting (Fig. 1, B-D, lane
112 8), yielded luciferase levels and RNA replication that was close to the wild type replicase.
113 Remarkably, a three-construct combination $1+2^{CA}3G+4$ mimicked this behavior (lane 9). However,
114 when 2/3 cleavage was allowed in the three-construct combination by transfecting 1+23G+4,

115 there was no evidence for RNA replication through luciferase activity or Northern blotting (lane
116 10). The implications of these results for replicase assembly are further examined and discussed
117 below.

118 **Formation of spherule structures in the absence of RNA template and replication.** The wild type
119 replicase can only form spherules in the presence of an RNA template but not in its absence. These
120 images are shown for comparison in Fig. 2 A and B. In the current work, we initially observed that
121 P1^2^3G4^{GAA}, which is replication-incompetent due to polymerase mutation (Fig. 1D, lane 11), was
122 capable of forming spherule structures both in the presence and in the absence of RNA template
123 with a seemingly equal efficiency (Fig. 2C and D). However, the appearance of these spherules was
124 distinct from those seen under replicating conditions. The novel structures were more
125 heterogeneous in size, and more irregularly shaped. We cannot exclude that cellular or plasmid-
126 derived RNAs could be unspecifically recruited to the invaginations in the absence of the viral
127 template. These novel membrane invaginations are clearly distinct from anything observed in non-
128 transfected cells, and for simplicity, we propose to call them inactive spherules, although the term
129 spherule-like structure could also be applied. Therefore, some alphavirus replicase protein
130 combinations can give rise to spherules in the absence of RNA, although under replicative
131 conditions the RNA contributes to the size and appearance of the spherules (20).

132 We next wanted to define the polyprotein requirements for spherule formation in
133 the absence of RNA. Not surprisingly, the inactivating polymerase mutation used in the first
134 experiment (Fig. 2C and D) did not influence spherule generation, and P1^2^3G4 containing an
135 active polymerase also yielded spherules (Fig. 2E). Totally cleavage-defective P12^{CA}3G4 did not
136 yield spherules in extensive searches made with this construct expressed at low levels (Fig. 2F),
137 and thus the cleavage of nsP4 was required. Secondly, uncleaved P123 (P12^{CA}3G) without the core

polymerase subunit nsP4 was not sufficient for spherule formation even if provided with a template (Fig. 2G), but P12^{CA}3G+4 readily gave rise to spherules in the absence of template (Fig. 2H). Therefore we concluded that the presence of individual nsP4 was required for spherule formation. P12^3G4 yielded spherules (Fig. 2I), indicating that the blocking of 2/3 cleavage was sufficient for spherule formation, compared to the wild type cleavable replicase that did not generate spherules in the absence of RNA template (Fig. 2B) or replication (14). Finally, the combination 1+2^{CA}3G+4 yielded spherule structures (Fig. 2J), although in this case they were rather few and difficult to find. The results with 1+23G+4 were somewhat ambiguous as individual structures resembling spherules were occasionally observed (Fig. 2K), while other samples were devoid of spherules. In conclusion, all the nsPs need to be present to generate spherules, and nsP4 needs to be cleaved off the remainder of the polyprotein, which can be provided as uncleaved P123, or as the combination of nsP1+uncleaved P23, with the former leading to more efficient spherule formation.

We note that it is not possible to provide numerical estimates of spherule frequencies, and so the previous observations report qualitative findings after thorough examination of several samples for each transfection. The reason for this inability is the extremely patchy distribution of spherules on cell surfaces, which can be seen in correlative fluorescence scanning electron microscopy (Fig. 3). Because large areas of the plasma membrane are devoid of spherules even in replication-positive or transfection-positive cells, in thin sections, such as shown in Fig. 2, it is necessary to screen multiple sections and large areas. Nevertheless, we are confident of the above findings, since e.g. P12^{CA}3G+4 in the absence of template consistently gives rather frequent clusters of spherules, and on the other hand, extensive efforts have been made to examine samples reported as spherule-negative.

nsP1+P23+nsP4 combination efficiently forms active replication complexes. The three-construct combination 1+2^{CA}3G+4, when provided with a template, gave luciferase activity and RNA replication at levels close to wild type replicase (Fig. 1C and D, lane 9). This combination with the template also yielded wild type spherules with a regular appearance and dot-like RNA staining (Fig. 4F). In contrast, the combination 1+23G+4 did not replicate to any extent (Fig. 1 C and D, lane 10). Altogether, this indicates that the three replication proteins nsP1, P23, and nsP4 constitute the minimal viral requirements for efficient assembly of replication complexes, and that the cleavage products of P23, that is nsP2 and nsP3, are no longer suitable for assembly.

We next assessed the localization of the key components required for replicase assembly. Uncleaved P23 (P2^{CA}3G) localized to cytoplasmic granular structures, with some general cytoplasmic background given by the nsP2 antibody (Fig. 4A). With a cleavable P23G construct, nsP3 localized in granules, whereas nsP2 was found diffusely either in the nucleus or in the cytoplasm (Fig. 4B). These localizations are typical of the proteins expressed separately, since SFV nsP2 has a nuclear localization signal, but remains cytoplasmic in a fraction of the cells, whereas nsP3 localizes to aggregations co-opting some of the components of cellular stress granules (21, 22). Thus, in uncleaved P23, the localization signals of nsP3 dominate those of nsP2. When nsP1 was co-expressed with P2^{CA}3G, the localization of the nsP3 signal started to change (Fig. 4C). This effect became more pronounced with the combination of 1+2^{CA}3G+4 (Fig. 4D), as P23G then in some regions displayed plasma membrane localization typical for nsP1 alone, and for the early replication complexes (Fig. 4D, inset).

To verify these results, P2^{CA}3G alone, and the combinations of 1+2^{CA}3G and 1+2^{CA}3G+4 were subjected to simple cell fractionation separating cytoplasmic fraction from membranes pelleting at 15,000 x g. nsP1 was always present almost exclusively in the membrane

184 fraction, as expected (23). P23G was soluble when expressed alone, but gained some membrane
185 association in the presence of nsP1, which was further enhanced by the addition of nsP4 (Fig. 4E,
186 upper panel). This experiment was extended by examining the nsP4-containing combinations
187 2^{CA}3G+4 and 1+ 2^{CA}3G+4 (Fig. 4E, lower panel). nsP4 had only a minor effect on the fractionation
188 of P23G. Notably, in the three-plasmid combination nsP4 became stabilized and was more
189 prominently present in the membrane fraction. In conclusion, P23 was recruited to membranes in
190 the presence of nsP1 and nsP4, likely due to assembly of entire replication complexes and some
191 spherule structures (see discussion).

192 **Partially uncleaved Sindbis virus nonstructural proteins generate spherules.** To analyze if these
193 phenomena would be applicable to other alphaviruses, a selected set of constructs were built for
194 SINV. These included P123 with protease-inactivating CA-substitution in nsP2 and eGFP fused to
195 nsP3, as well as the wild type, cleavable version of this polyprotein. nsP4 was usually produced as
196 a separate protein utilizing ubiquitin fusion (Fig. 5A). The proteins were first analyzed by Western
197 blotting, in which uncleaved P123 gave rise to the expected large-molecular mass band (Fig. 5B). In
198 luciferase assay, all polyprotein constructs were active, when all four proteins were expressed
199 together with a template. Somewhat surprisingly, the CA-substitution in nsP2 did not reduce
200 luciferase expression, and the counts were generally two orders of magnitude above the
201 background of template only control (Fig. 5C). The polyprotein plasmid-transfected cells were then
202 studied in EM, both with and without template expression. Similarly to SFV, the SINV P12^{CA}3+4
203 combination producing uncleaved P123 was able to form plentiful spherule structures even in the
204 absence of template (Fig. 5Di), but spherules were very rare when P123 was cleavable (Fig. 5Dii).
205 As a comparison, a sample with template was included, verifying the efficient active spherule
206 formation with the uncleaved P123 together with nsP4 (Fig. 5Diii). The analysis of proteins
207 localizations showed similar behavior as with SFV, i.e. nsP2 and nsP3 were detected diffusely, and

were to some extent seen on the plasma membrane, when nsP1-3 were expressed as an uncleavable polyprotein P12^{CA}3G (Fig. 5E, upper row). When the polyprotein was cleavable, nsP2 distributed throughout the cytoplasm and nsP3 was found exclusively in granules (Fig. 5E, lower row), in spite of the possible presence of multiple forms of nsP3 (Fig. 5B). We note that in a previous study it was reported that the SINV combination of uncleaved P123+4 in the absence of template did not yield spherules (24). We attribute our current clearly positive result to the use of CLEM technique, with which we can exclusively focus on those cells that express the polyprotein, as detected by fluorescence.

Discussion

We showed here that membrane invaginations can be generated by the alphavirus replicase in the absence of RNA replication or RNA template. All four nsPs are necessary, such that nsP4 has to be cleaved from the other proteins (or be produced separately), but P123 or at least P23 needs to remain uncleaved. These requirements for replication spherule formation can be compared with brome mosaic virus (BMV), which is a member of the alphavirus-like superfamily and thus its replication proteins are distantly related to their alphavirus counterparts (25). The two replication proteins of BMV are produced from separate RNAs and there is no proteolytic cleavage. Interestingly, BMV 1a protein alone can form spherules very efficiently on its own in the absence of the core polymerase subunit 2a (26). 1a contains RNA capping enzyme and RNA helicase domains corresponding to alphavirus nsP1 and the N-terminal domain of nsP2. No gross morphological differences of BMV spherules in the presence and absence of RNA template have been reported, but specific mutations in 1a can alter the size and abundance of the spherules (27, 28). In contrast, the size of alphavirus spherules is determined by the length of the RNA template

(20), for which no effect has been reported in the case of BMV spherules. The order of events during spherule formation has not been established, but for BMV it has been speculated that RNA could be transported to the spherules after they have been formed (29). We think that such a scenario is unlikely in alphaviruses, and have proposed that in wild type virus RNA synthesis and spherule formation would be linked (20). A third example of spherule formation is provided by the unrelated tombusviruses, in which RNA also determines spherule size (30).

The function of alphavirus replication complexes requires all the four nsPs. This work shows that the assembly of spherules structures even in the absence of template RNA also requires all of these proteins. In particular, nsP4 needs to be cleaved, whereas efficient spherule formation was achieved only when P123 remained uncleaved. This configuration corresponds exactly to the early alphavirus polymerase synthesizing predominantly negative-strand RNA (12). It is thought that both in BMV and in alphavirus replication complexes the core polymerase component is present in smaller quantities compared to the other viral protein(s) (26, 31). It is therefore somewhat surprising that alphavirus nsP4 is absolutely required for spherule formation, whereas BMV 2a is not. nsP4 may for instance facilitate the proper interactions of the other domains within the alphavirus replicase that are not found in BMV proteins. This possibility could be supported by the result that nsP4 seemed to increase the membrane recruitment of P23 in the presence of the membrane anchoring component nsP1. Alternatively, nsP4 could be necessary for the recruitment of host factors that promote spherule formation.

In the absence of RNA, uncleaved P123+nsP4 generated spherules more efficiently than nsP1+uncleaved P23+nsP4. In presence of RNA the latter combination still efficiently assembled replication complexes, but cleavable P23 did not. Earlier results also support an essential role for the precursor P23, since mutations in nsP1 and nsP4 can complement those in nsP2 or nsP3, but genetically nsP2 and nsP3 form a single cistron (32). Secondly, in prior

255 experiments the attempt to express cleavable SINV P23 together with the other replicase
256 components also failed to yield RNA replication (11). On the other hand, uncleaved P23 can
257 function quite well for replication, as shown here and earlier (13). The fact that alphavirus
258 replicase can be assembled from three virus-specific components suggests that these proteins
259 might be separately purified for assembly experiments. While they are prone to aggregation in
260 expression systems, progress has been reported with all: the capping enzyme nsP1, the
261 polymerase nsP4 and large portions of the P23 precursor (33-35).

262 With the expression of replication proteins alone, spherule-like membrane
263 invaginations could be detected but their sizes were variable and often small in the cases where
264 no template was included. This is in agreement with our previous data, where we measured
265 spherule sizes and showed that the size is dependent on the template length (20). Thus, it seems
266 that the proteins themselves are enough for the induction of membranous structures in various
267 sizes, but only if they are not completely cleaved and have enough time to interact and form a
268 complex. It is also possible that only in correct conformation the replicase proteins are able to
269 interact with cellular factors that are present at the replication complexes (36-38). Although these
270 host proteins promote virus replication and interact with nsP3, their specific actions are not
271 understood. The current results provide the means to specifically assay spherule formation
272 independently of RNA replication. Thus, experiments can now be made to clarify whether the host
273 factors contribute to membrane deformation, as proposed for the membrane-curving protein
274 amphiphysin (37), or to other aspects of replicase assembly or function.

275

276 **Materials and methods**

277 **Cells and cell fractionation.** BSR T7/5 cells, a derivative of BHK cells stably expressing T7 RNA
278 polymerase (39), were cultured in Dulbecco's modified Eagle's medium (DMEM) supplemented
279 with 10% foetal bovine serum, 2 mM L-glutamine, 100 U/ml penicillin and 100 µg/ml streptomycin
280 further supplemented with 2% bacto tryptose phosphate broth, non-essential amino acids, and 1
281 mg/ml G418 for selection of T7 polymerase expression. For fractionation, cells were transfected
282 with the indicated protein combinations on 10 cm dishes using Lipofectamine™ LTX (Invitrogen).
283 At 16 hours post transfection, cells were harvested, washed with phosphate-buffered saline and
284 swollen in 10 mM Tris/HCl (pH 8.0) and 10 mM NaCl, supplemented with Pierce^{TM} Protease
285 Inhibitors (Thermo Fisher Scientific). Cells were disrupted in a Dounce homogenizer with 30
286 strokes. Post-nuclear supernatant was prepared by removing the nuclei and intact cells by
287 centrifugation at 500 x g for 10 min. The post-nuclear supernatant was further centrifuged at
288 15,000 x g for 20 min to obtain membrane (P15) and supernatant (S15) fractions.
289
290 **Plasmid constructs for SFV.** Plasmids encoding the wild-type replicase polyprotein P123Z4 (Z
291 indicates fluorescent protein ZsGreen), the polyprotein with inactivated polymerase P123Z4^{GAA}
292 and the polyprotein with mutated processing sites P1^2^3Z4 as well as ubi-nsP4, have been
293 described previously (14). To obtain processing deficient replicase polyprotein with inactive RNA
294 polymerase (P1^2^3Z4^{GAA}), the mutated fragment of nsP4 was transferred from plasmid
295 P123Z4^{GAA} by using Bsu36I and BamHI restriction sites. To obtain completely processing-deficient
296 replicase polyprotein (P12^{CA}3Z4), nsP4 was inserted into P12^{CA}3Z construct (16) by using the same
297 restriction sites. In order to replace ZsGreen with eGFP, the eGFP was first PCR-amplified and
298 cloned into the naturally occurring XhoI-site in SFV replicon plasmid pSFV1 (40). The eGFP
299 containing fragment was then transferred to P123Z4 and P123Z4^{GAA} by using the restriction sites
300 Bsu36I with BamHI or NotI, respectively. Similarly, eGFP was cloned into P12^{CA}3Z4, P1^2^3Z4 and

P1^2^3Z4^{GAA} with Bsu36I and NotI. The construct P12^3G4 was created by transferring the SacI – Bsu36I fragment, including the cleavage-defective site between nsP2 and nsP3, from P1^2^3Z4 to P123G4. In order to replace ZsGreen with eGFP in P12Z3 and P1^2^3Z (14), the Bsu36I and AgeI digested fragment of nsP3-eGFP was transferred from P123G4 to P12Z3 and P1^2^3Z. The nsP1-expressing construct was created using PCR amplification. A forward primer (5´-AACACAGCGAAACACTAACACGA-3´) and a reverse primer (5´-TAGGTTAATTAA**TTA**TGCACCTGCGTGATACTCT-3´) were used, the latter designed to carry a stop codon (in bold) followed by PacI restriction site (underlined). The fragment was used to replace the MscI - PacI region of P123Z4, thus deleting nsP2-4 coding regions. ubi-nsP23G and ubi-nsP2^{CA}3G were constructed by cloning a fragment of ubi-nsP2, containing a similar ubiquitin fusion as nsP4 (14), with NcoI and SacI into P123G and P12^{CA}3G, thus removing nsP1 from both. Previously described template constructs Tshort (14) and Tmed_Vis (16) were used.

Plasmid constructs for SINV. All constructs were based on the TOTO1101 isolate of SINV; the corresponding infectious clone plasmid (41) was used as the source of fragments for subcloning procedures. A plasmid expressing wild type P1234 under the control of bacteriophage T7 RNA polymerase promoter was constructed as described for the equivalent chikungunya virus construct (42), except that the sequence was not codon-optimized and that sequences from human beta actin, hepatitis delta virus ribozyme or T7 terminator were not included. The obtained expression plasmid was designated P1234-SINV. In plasmid P123G, lacking nsP4 region, eGFP (flanked with Gly-Gly dipeptide linkers) insertion after codon 1734 of P123 was achieved by replacement of the SfiI-PacI fragment of P1234-SINV with a synthetic DNA fragment (Genscript). In order to obtain a plasmid for expression of SINV P123 without eGFP insertion, the corresponding sequence was removed by SpeI digestion. Constructs P12^{CA}3-EGFP-SINV and P12^{CA}3-SINV, harboring a mutation substituting Cys 1021 residue (the catalytic residue of nsP2 protease) by Ala

residue, were obtained using PCR-based mutagenesis and subcloning procedures. The construct designated as ubi-nsP4-SINV was obtained by replacement of PflMI-EcoRI restriction fragment of P1234-SINV with a synthetic fragment (Genscript) consisting of the downstream part of encephalomyocarditis virus internal ribosome entry site followed by ubiquitin and sequence encoding the SINV nsP4 N-terminal region.

The plasmid encoding a truncated RNA template for SINV replicase was constructed as follows. The basic expression cassette was obtained as synthetic DNA (Genscript) and consisted of the following parts: i) promoter for bacteriophage T7 RNA polymerase followed by 257 5' residues of SINV genome, ii) fragment corresponding to SINV subgenomic RNA promoter (residues -76 to 63, with respect to the beginning of subgenomic RNA), iii) 3' UTR of SINV (322 residues from the 3' end of SINV genome) followed by a poly(A) sequence of 30 residues, the negative strand ribozyme of hepatitis delta virus and T7 terminator. Elements I and II, as well as elements II and III were separated by short polylinkers containing unique restriction sites. Sequence encoding *Renilla* luciferase reporter was PCR amplified and cloned into the polylinker between elements I and II, such that the coding sequence for an N-terminal fragment of SINV nsP1 was in frame with *Renilla* luciferase. Sequence encoding for Tomato marker protein was PCR amplified and cloned into the polylinker between elements II and III, and the obtained plasmid was designated SINV-Rluc-Tom. The sequences of all constructs were verified by Sanger sequencing and are available from the authors upon request.

Western blotting. Cells were transfected with plasmids by using Lipofectamine™ LTX reagent (Invitrogen) according to manufacturer's instructions and incubated for 16 h. Total cell lysates were fractionated on 10% SDS-polyacrylamide gels followed by transfer to Hybond-ECL (Amersham Biosciences). Filters were blocked against nonspecific binding using 5% non-fat dry

milk powder, and probed with antibodies specific for individual SFV or SINV nsPs. Equal loading was confirmed by probing the same filter with an antibody for β-actin (Sigma-Aldrich). Signals were obtained by incubating the filters with secondary antibodies IRDye®800CW donkey anti-rabbit IgG (Li-cor Biosciences) and Alexa Fluor 680 anti-mouse IgG (Invitrogen) and scanning the filters with Odyssey system (Li-cor).

Luciferase assay. Transfections for luciferase assay were done on 96-well plates for 16 hours and measured as previously described (14) by using Promega's luciferase assay system according to the manufacturer's instructions.

Confocal microscopy. BSR cells were grown on coverslips and transfected with different construct combinations by using Lipofectamine™ LTX according to manufacturer's instructions. Cells were fixed after 16 h with 4% paraformaldehyde for 20 minutes, washed three times with PBS and quenched with 50 mM NH_4Cl. After permeabilization with 0.1% Triton X-100, samples were incubated with primary antibodies for 1h, washed three times with PBS and incubated with appropriate secondary antibodies for 1 h. After careful washes, samples were mounted with ProLong® Gold containing 4', 6-diamidino-2-phenylindole (DAPI) (Molecular Probes). Cells were analyzed with Leica TCS SP5II HCS A confocal microscope using HCX PL APO 63x/1.2W Corr/0.17 CS (water) objective. Confocal images were analyzed by using either BioImageXD (43) or ImageJ (National Institutes of Health, MD) software.

CLEM. BSR cells were grown either on MatTek or ibidi dishes with glass bottom and grid, and transfected with indicated combinations of SFV or SINV constructs by using Lipofectamine™ LTX. All CLEM samples were fixed with 2% glutaraldehyde in 0.1 M sodium-cacodylate buffer for 30 min at room temperature and washed with the buffer three times. Cells were immediately imaged with Leica TCS SP5II HCS A confocal microscope using HC PL APO 20x/0,7 CS (air) objective.

371 Fluorescence mode was used to obtain images from transfection-positive cells and differential
372 interference contrast (DIC) mode to image the grid of the dish. Samples were then prepared for
373 transmission electron microscopy. Briefly, samples were stained with reduced buffered osmium
374 tetroxide and uranyl acetate and processed for flat embedding and ultrathin sectioning as
375 previously described (18). Positive cells were relocated in electron microscopy based on previously
376 taken fluorescence and DIC images and imaged with Jeol JEM-1400 and (80 kV) and bottom-
377 mounted camera Gatan Orius SC 1000B.

378 For scanning electron microscopy, cells were grown and transfected on ibidi dishes
379 and processed as above until ethanol dehydration. After that, cells were covered with
380 hexamethyldisilazane (Fluka) and were left to dry o/n in a fume hood. Samples were mounted on
381 aluminum specimen tubs, coated with platinum sputter and imaged with FEI Quanta 250 Field
382 Emission Gun scanning electron microscope (10 kV).

383 **RNA isolation and Northern blotting.** RNA isolation and Northern blotting were performed as
384 previously described (20). Briefly, 16 h post transfection, BSR cells were lysed and collected with
385 TRIsure reagent (Bioline) followed by RNA isolation according to manufacturer's instructions
386 except that an additional phenol (pH 5.0)/ chloroform extraction was performed prior to
387 precipitation. 2 micrograms of total RNA was fractionated on a denaturating 1% agarose gel, and
388 transferred to positively charged Amersham Hybond-N+ nylon filter (GE Healthcare) by capillary
389 blotting overnight. RNA was cross-linked to the membrane with Stratalinker (Stratagene). [^{32}P]-
390 labeled antisense probes for (+)strand and (-)strand RNA detection recognized the *Renilla*
391 luciferase gene present in template constructs. Prehybridization and hybridization were
392 performed as described (20).

393

Acknowledgements. We thank Mervi Lindman and Arja Strandell for excellent technical assistance with EM samples. This study was funded by Academy of Finland (grant 265997 to TA) and Estonian Research Council (grant IUT 20-27 to AM).

Figure legends

Fig. 1. Ability of partially cleaved SFV replicases to synthesize RNA. A) Schematic of the SFV replicase and template expressing constructs used for analysis. The replicase is shown as a single construct under T7 promoter, but note that in some experiments it is divided to 2 or 3 fragments, each expressed from a separate plasmid. The sites of mutations inactivating the nsP2 protease, nsP4 polymerase or destroying the cleavage sites (present in different constructs) are shown. The insertion of eGFP (denoted G in polyprotein constructs) to nsP3 is indicated. The template Tshort (14) contains the regions of viral RNA necessary for replication and expresses the *Renilla* luciferase enzyme. IRES, internal ribosome entry site; SGP, subgenomic promoter; Rz, ribozyme. B) Expression of the nonstructural proteins from the obtained constructs (indicated at the top) after transfection, as analyzed by Western blotting with antibody against nsP3. As a loading control, β-actin elevel in the samples is shown at the bottom. The bands of nsP3-containing polypeptides are marked. C) Luciferase activity in cell extracts 16 h after transfection of the polyprotein constructs together with template Tshort. Transfections were carried out in quadruplicate wells; the values represent average ± standard deviation. D) Negative- (upper panel) and positive-strand (lower panel) RNA detected by Northern blotting. The arrows indicate the size of the template Tshort. Incomplete termination of T7 transcription yields larger bands, some of which appear to be replicating, but the nature of these RNAs remain uncharacterized (20). In panels B-D, a

representative experiment is shown, and the constructs are shown in the same order in the three panels.

Fig. 2. Visualization of spherule structures. Representative images of thin sections from cells transfected with the indicated constructs are shown. All the images are from transfection-positive cells based on eGFP fluorescence. The scale bar is 200 nm. In panel A, a few representative spherule structures have been pointed out with arrowheads.

Fig. 3. Spherules on the cell surface visualized from the outside. Cells transfected with the indicated constructs were processed for scanning electron microscopy, and fluorescence-positive cells were visualized at the EM level. Spherules are seen as small white dots. The scale bars are 3 μm in the left panels, and 500 nm in the enlarged right panels.

Fig. 4. Experiments with P23. A-D) Localization of replicase proteins. Cells were transfected with the constructs indicated on the left and protein localization was detected at 16 h post transfection by using antibodies against nsP1 or nsP2, or by using the autofluorescence of nsP3-eGFP fusion protein, as indicated in the individual panels. Scale bars 10 μm. In the insets, a merged color image of the indicated region is shown to visualize co-localization. E) Fractionation of cells expressing the protein combinations indicated at the top. The post-nuclear supernatant fraction (PNS) was fractionated to membranes pelleting at 15,000 x g (P15) and the remaining supernatant (S15). The fractions were analyzed by Western blotting with antibodies against nsPs, as indicated on the

right. β-actin was used as a loading control. F) Visualization of spherules in a cell expressing the three-protein combination 1+2^{CA}3G+4 together with template. Scale bar 200 nm.

Fig. 5. Characterization of partially uncleaved SINV replicases. A) Schematic of the SINV replicase illustrating the expression of P123 and nsP4 from separate constructs. The template used contains both *Renilla* luciferase and the Tomato fluorescent protein genes. IRES, internal ribosome entry site; SGP, subgenomic promoter; Rz, ribozyme. B) Expression of SINV proteins from the constructs (indicated at the top) after transfection, as analyzed by Western blotting with antibody against SINV nsP3. As a loading control, β-actin expression in the samples is shown at the bottom. The expected sizes of nsP3-containing bands are marked on the right. In cleavable constructs, several bands are actually detected, and there is a prominent unspecific band present in all samples (marked with an asterisk). C) Luciferase activity in cell extracts 16 h after transfection of the polyprotein constructs together with the template. Transfections were carried out in quadruplicate wells; the values represent average ± standard deviation. D) Representative EM images of thin sections from cells transfected with the indicated constructs are shown. Scale bars 200 nm. E) Localization of nsP2 and nsP3-containing proteins in cells transfected with the indicated construct combinations. The detection of nsP2 (in red) was performed with a polyclonal antibody and nsP3 (in green) utilizing eGFP-fusion. Scale bars 10 µm.

References

1. ***Griffin DE.*** *2013. Alphaviruses, p 651-686. In Knipe DM, Howley PM, Cohen JI, Griffin DE, Lamb RA, Martin MA, Racaniello VR, Roizman B (ed), Fields Virology, 6th ed, vol 1. Lippincott Williams & Wilkins, Philadelphia, PA.*
2. ***Froshauer S, Kartenbeck J, Helenius A.*** *1988. Alphavirus RNA replicase is located on the cytoplasmic surface of endosomes and lysosomes. J Cell Biol.* ***107****:2075-2086.*

3. **Kujala P, Ikaheimonen A, Ehsani N, Vihinen H, Auvinen P, Kääriäinen L.** *2001. Biogenesis of the Semliki Forest virus RNA replication complex. J Virol.* ***75****:3873-3884.*
4. **Spuul P, Balistreri G, Kääriäinen L, Ahola T.** *2010. Phosphatidylinositol 3-kinase-, actin-, and microtubule-dependent transport of Semliki Forest Virus replication complexes from the plasma membrane to modified lysosomes. J Virol.* ***84****:7543-7557.*
5. **Paul D, Bartenschlager R.** *2013. Architecture and biogenesis of plus-strand RNA virus replication factories. World J Virol.* ***2****:32-48.*
6. **Neufeldt CJ, Joyce MA, Van Buuren N, Levin A, Kirkegaard K, Gale M, Jr., Tyrrell DL, Wozniak RW.** *2016. The Hepatitis C Virus-Induced Membranous Web and Associated Nuclear Transport Machinery Limit Access of Pattern Recognition Receptors to Viral Replication Sites. PLoS Pathog.* ***12****:e1005428.*
7. **Salonen A, Ahola T, Kääriäinen L.** *2005. Viral RNA replication in association with cellular membranes. Curr Top Microbiol Immunol.* ***285****:139-173.*
8. **Knoops K, Kikkert M, Worm SH, Zevenhoven-Dobbe JC, van der Meer Y, Koster AJ, Mommaas AM, Snijder EJ.** *2008. SARS-coronavirus replication is supported by a reticulovesicular network of modified endoplasmic reticulum. PLoS Biol.* ***6****:e226.*
9. **Welsch S, Miller S, Romero-Brey I, Merz A, Bleck CK, Walther P, Fuller SD, Antony C, Krijnse-Locker J, Bartenschlager R.** *2009. Composition and three-dimensional architecture of the dengue virus replication and assembly sites. Cell Host Microbe.* ***5****:365-375.*
10. **Lemm JA, Rice CM.** *1993. Roles of nonstructural polyproteins and cleavage products in regulating Sindbis virus RNA replication and transcription. J Virol.* ***67****:1916-1926.*
11. **Lemm JA, Rice CM.** *1993. Assembly of functional Sindbis virus RNA replication complexes: requirement for coexpression of P123 and P34. J Virol.* ***67****:1905-1915.*
12. **Lemm JA, Rumenapf T, Strauss EG, Strauss JH, Rice CM.** *1994. Polypeptide requirements for assembly of functional Sindbis virus replication complexes: a model for the temporal regulation of minus- and plus-strand RNA synthesis. EMBO J.* ***13****:2925-2934.*
13. **Shirako Y, Strauss JH.** *1994. Regulation of Sindbis virus RNA replication: uncleaved P123 and nsP4 function in minus-strand RNA synthesis, whereas cleaved products from P123 are required for efficient plus-strand RNA synthesis. J Virol.* ***68****:1874-1885.*
14. **Spuul P, Balistreri G, Hellström K, Golubtsov AV, Jokitalo E, Ahola T.** *2011. Assembly of alphavirus replication complexes from RNA and protein components in a novel trans-replication system in mammalian cells. J Virol.* ***85****:4739-4751.*
15. **Hellström K, Kallio K, Meriläinen HM, Jokitalo E, Ahola T.** *2016. Ability of minus strands and modified plus strands to act as templates in Semliki Forest virus RNA replication. J Gen Virol.* ***97****:1395-1407.*
16. **Kallio K, Hellström K, Jokitalo E, Ahola T.** *2016. RNA Replication and Membrane Modification Require the Same Functions of Alphavirus Nonstructural Proteins. J Virol.* ***90****:1687-1692.*
17. **Vasiljeva L, Merits A, Golubtsov A, Sizemskaja V, Kääriäinen L, Ahola T.** *2003. Regulation of the sequential processing of Semliki Forest virus replicase polyprotein. J Biol Chem.* ***278****:41636-41645.*
18. **Hellström K, Vihinen H, Kallio K, Jokitalo E, Ahola T.** *2015. Correlative light and electron microscopy enables viral replication studies at the ultrastructural level. Methods.* ***90****:49-56.*
19. **Frolova E, Gorchakov R, Garmashova N, Atasheva S, Vergara LA, Frolov I.** *2006. Formation of nsP3-specific protein complexes during Sindbis virus replication. J Virol.* ***80****:4122-4134.*
20. **Kallio K, Hellström K, Balistreri G, Spuul P, Jokitalo E, Ahola T.** *2013. Template RNA length determines the size of replication complex spherules for Semliki Forest virus. J Virol.* ***87****:9125-9134.*
21. **Panas MD, Varjak M, Lulla A, Eng KE, Merits A, Karlsson Hedestam GB, McInerney GM.** *2012. Sequestration of G3BP coupled with efficient translation inhibits stress granules in Semliki Forest virus infection. Mol Biol Cell.* ***23****:4701-4712.*
22. **Peränen J, Rikkonen M, Liljestrom P, Kääriäinen L.** *1990. Nuclear localization of Semliki Forest virus-specific nonstructural protein nsP2. J Virol.* ***64****:1888-1896.*
23. **Laakkonen P, Ahola T, Kääriäinen L.** *1996. The effects of palmitoylation on membrane association of Semliki forest virus RNA capping enzyme. J Biol Chem.* ***271****:28567-28571.*

24. **Frolova EI, Gorchakov R, Pereboeva L, Atasheva S, Frolov I.** *2010. Functional Sindbis virus replicative complexes are formed at the plasma membrane. J Virol.* ***84****:11679-11695.*
25. **Kääriäinen L, Ahola T.** *2002. Functions of alphavirus nonstructural proteins in RNA replication. Prog Nucleic Acid Res Mol Biol.* ***71****:187-222.*
26. **Schwartz M, Chen J, Janda M, Sullivan M, den Boon J, Ahlquist P.** *2002. A positive-strand RNA virus replication complex parallels form and function of retrovirus capsids. Mol Cell.* ***9****:505-514.*
27. **Liu L, Westler WM, den Boon JA, Wang X, Diaz A, Steinberg HA, Ahlquist P.** *2009. An amphipathic alpha-helix controls multiple roles of brome mosaic virus protein 1a in RNA replication complex assembly and function. PLoS Pathog.* ***5****:e1000351.*
28. **Wang X, Lee WM, Watanabe T, Schwartz M, Janda M, Ahlquist P.** *2005. Brome mosaic virus 1a nucleoside triphosphatase/helicase domain plays crucial roles in recruiting RNA replication templates. J Virol.* ***79****:13747-13758.*
29. **Kopek BG, Settles EW, Friesen PD, Ahlquist P.** *2010. Nodavirus-induced membrane rearrangement in replication complex assembly requires replicase protein a, RNA templates, and polymerase activity. J Virol.* ***84****:12492-12503.*
30. **Kovalev N, de Castro Martin IF, Pogany J, Barajas D, Pathak K, Risco C, Nagy PD.** *2016. Role of Viral RNA and Co-opted Cellular ESCRT-I and ESCRT-III Factors in Formation of Tombusvirus Spherules Harboring the Tombusvirus Replicase. J Virol.* ***90****:3611-3626.*
31. **de Groot RJ, Rumenapf T, Kuhn RJ, Strauss EG, Strauss JH.** *1991. Sindbis virus RNA polymerase is degraded by the N-end rule pathway. Proc Natl Acad Sci U S A.* ***88****:8967-8971.*
32. **Wang YF, Sawicki SG, Sawicki DL.** *1994. Alphavirus nsP3 functions to form replication complexes transcribing negative-strand RNA. J Virol.* ***68****:6466-6475.*
33. **Li C, Guillen J, Rabah N, Blanjoie A, Debart F, Vasseur JJ, Canard B, Decroly E, Coutard B.** *2015. mRNA Capping by Venezuelan Equine Encephalitis Virus nsP1: Functional Characterization and Implications for Antiviral Research. J Virol.* ***89****:8292-8303.*
34. **Rubach JK, Wasik BR, Rupp JC, Kuhn RJ, Hardy RW, Smith JL.** *2009. Characterization of purified Sindbis virus nsP4 RNA-dependent RNA polymerase activity in vitro. Virology.* ***384****:201-208.*
35. **Shin G, Yost SA, Miller MT, Elrod EJ, Grakoui A, Marcotrigiano J.** *2012. Structural and functional insights into alphavirus polyprotein processing and pathogenesis. Proc Natl Acad Sci U S A.* ***109****:16534-16539.*
36. **Kim DY, Reynaud JM, Rasalouskaya A, Akhrymuk I, Mobley JA, Frolov I, Frolova EI.** *2016. New World and Old World Alphaviruses Have Evolved to Exploit Different Components of Stress Granules, FXR and G3BP Proteins, for Assembly of Viral Replication Complexes. PLoS Pathog.* ***12****:e1005810.*
37. **Neuvonen M, Kazlauskas A, Martikainen M, Hinkkanen A, Ahola T, Saksela K.** *2011. SH3 domain-mediated recruitment of host cell amphiphysins by alphavirus nsP3 promotes viral RNA replication. PLoS Pathog.* ***7****:e1002383.*
38. **Schulte T, Liu L, Panas MD, Thaa B, Dickson N, Gotte B, Achour A, McInerney GM.** *2016. Combined structural, biochemical and cellular evidence demonstrates that both FGDF motifs in alphavirus nsP3 are required for efficient replication. Open Biol.* ***6****.*
39. **Buchholz UJ, Finke S, Conzelmann KK.** *1999. Generation of bovine respiratory syncytial virus (BRSV) from cDNA: BRSV NS2 is not essential for virus replication in tissue culture, and the human RSV leader region acts as a functional BRSV genome promoter. J Virol.* ***73****:251-259.*
40. **Liljeström P, Garoff H.** *1991. A new generation of animal cell expression vectors based on the Semliki Forest virus replicon. Biotechnology (N Y).* ***9****:1356-1361.*
41. **Rice CM, Levis R, Strauss JH, Huang HV.** *1987. Production of infectious RNA transcripts from Sindbis virus cDNA clones: mapping of lethal mutations, rescue of a temperature-sensitive marker, and in vitro mutagenesis to generate defined mutants. J Virol.* ***61****:3809-3819.*
42. **Utt A, Quirin T, Saul S, Hellström K, Ahola T, Merits A.** *2016. Versatile Trans-Replication Systems for Chikungunya Virus Allow Functional Analysis and Tagging of Every Replicase Protein. PLoS One.* ***11****:e0151616.*

43. ***Kankaanpaa P, Paavolainen L, Tiitta S, Karjalainen M, Paivarinne J, Nieminen J, Marjomaki V, Heino J, White DJ.*** *2012. BioImageXD: an open, general-purpose and high-throughput image-processing platform. Nat Methods.* ***9****:683-689.*

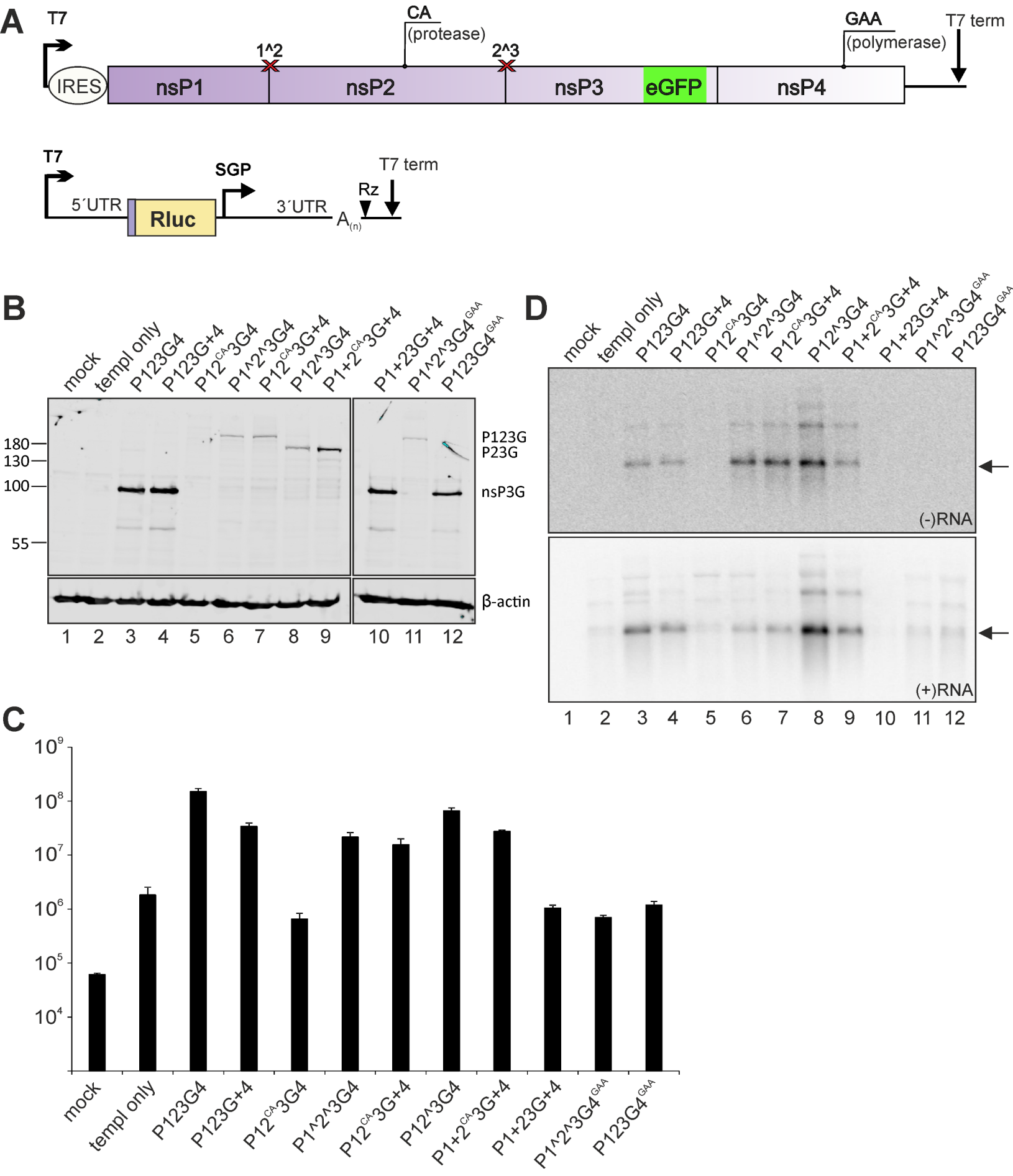
A
T7
IRES
nsP1
1^2
nsP2
CA
(protease)
2^3
nsP3
eGFP
nsP4
GAA
(polymerase)
T7 term
T7
5´UTR
Rluc
SGP
3´UTR
A(n)
Rz
T7 term
B
mock
templ only
P123G4
P123G+4
P12CA3G4
P1^2^3G4
P12CA3G+4
P12^3G4
P1+2CA3G+4
P1+23G+4
P1^2^3G4GAA
P123G4GAA
180
130
100
55
P123G
P23G
nsP3G
β-actin
1 2 3 4 5 6 7 8 9 10 11 12
D
mock
templ only
P123G4
P123G+4
P12CA3G4
P1^2^3G4
P12CA3G+4
P12^3G4
P1+2CA3G+4
P1+23G+4
P1^2^3G4GAA
P123G4GAA
(-)RNA
(+)RNA
1 2 3 4 5 6 7 8 9 10 11 12
C
10^9
10^8
10^7
10^6
10^5
10^4
mock
templ only
P123G4
P123G+4
P12CA3G4
P1^2^3G4
P12CA3G+4
P12^3G4
P1+2CA3G+4
P1+23G+4
P1^2^3G4GAA
P123G4GAA

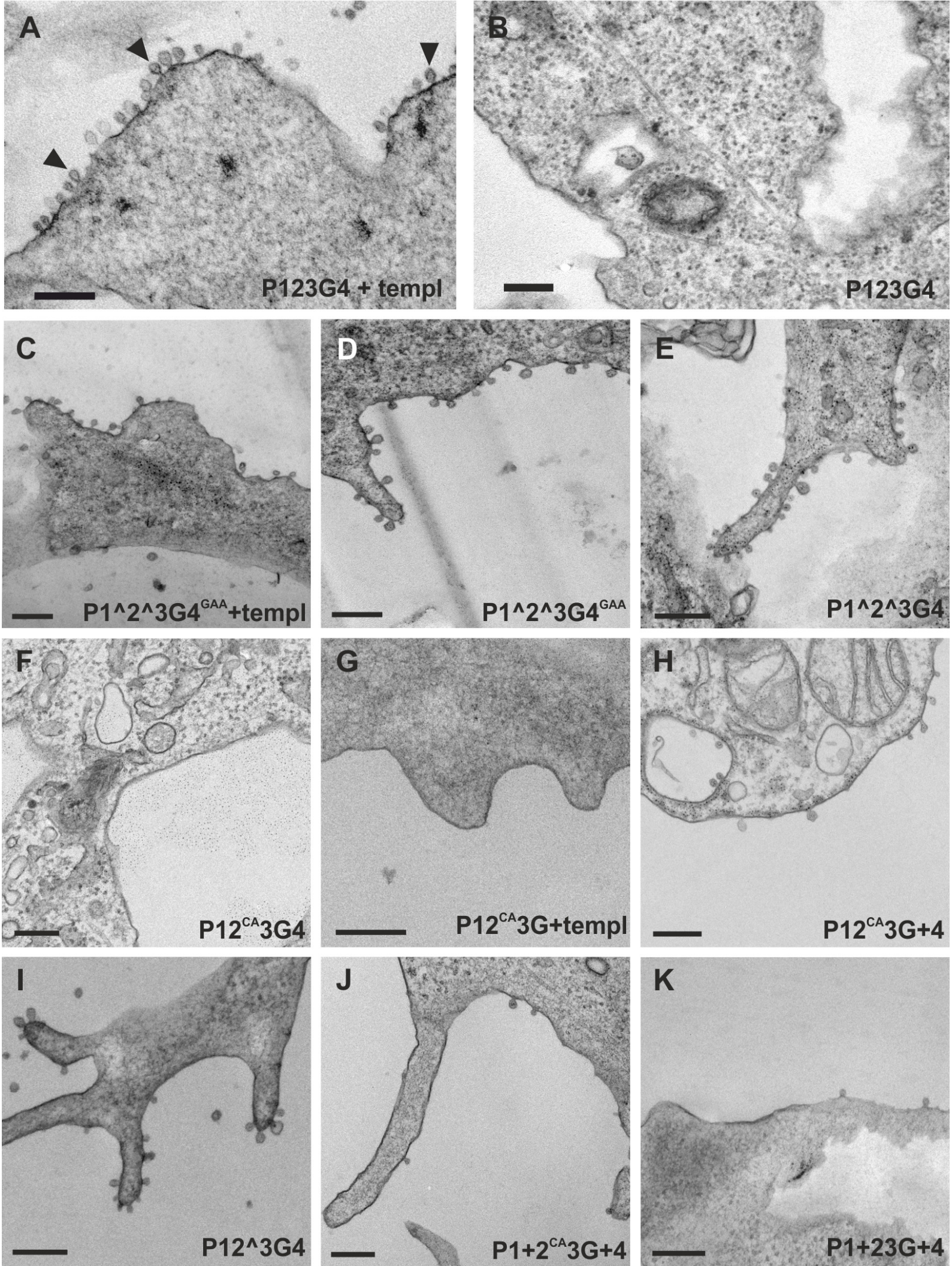
A
P123G4 + templ
B
P123G4
C
P1^2^3G4GAA+templ
D
P1^2^3G4GAA
E
P1^2^3G4
F
P12CA3G4
G
P12CA3G+templ
H
P12CA3G+4
I
P12^3G4
J
P1+2CA3G+4
K
P1+23G+4

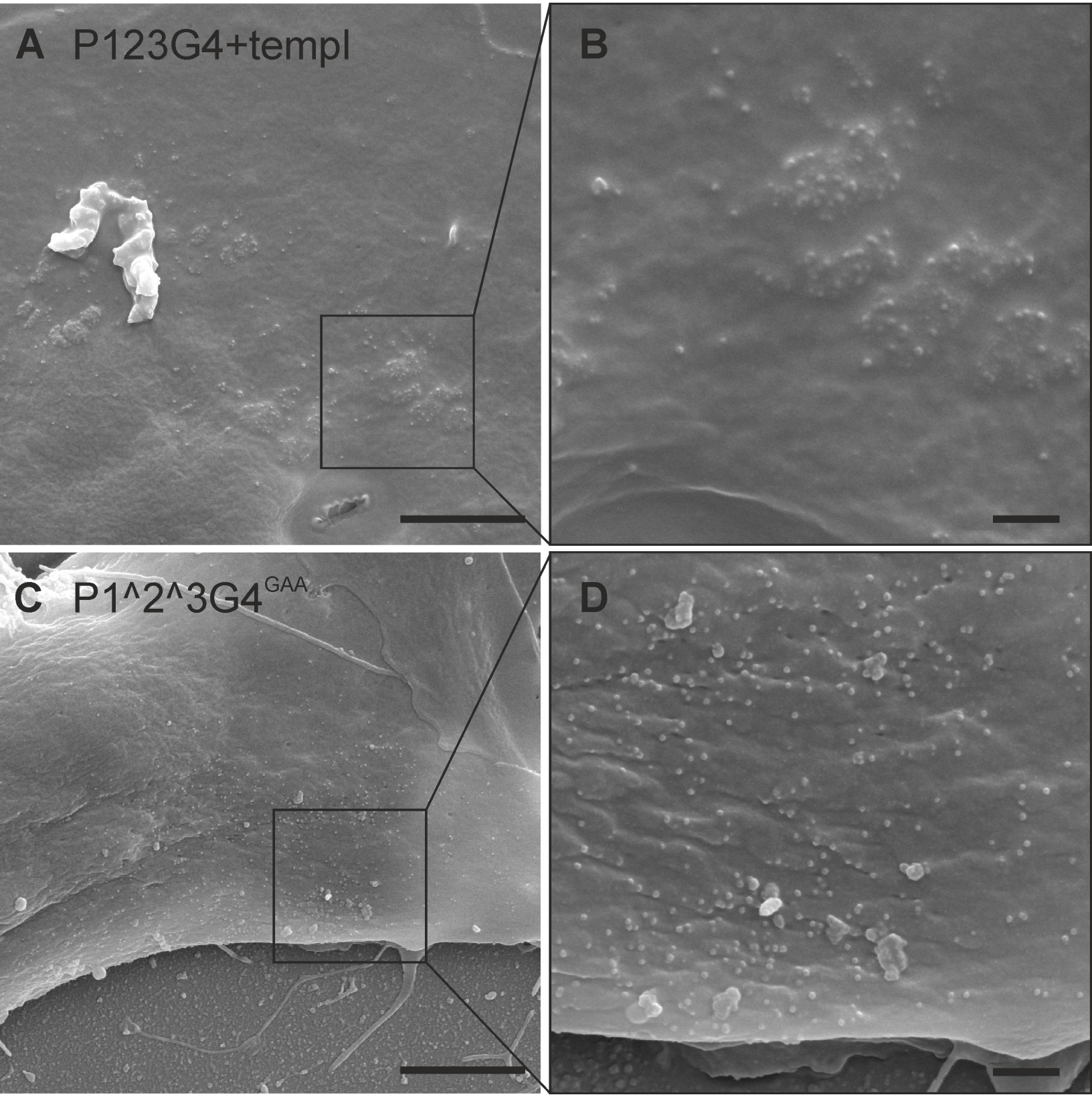
A P123G4+templ
B
C P1^2^3G4GAA
D

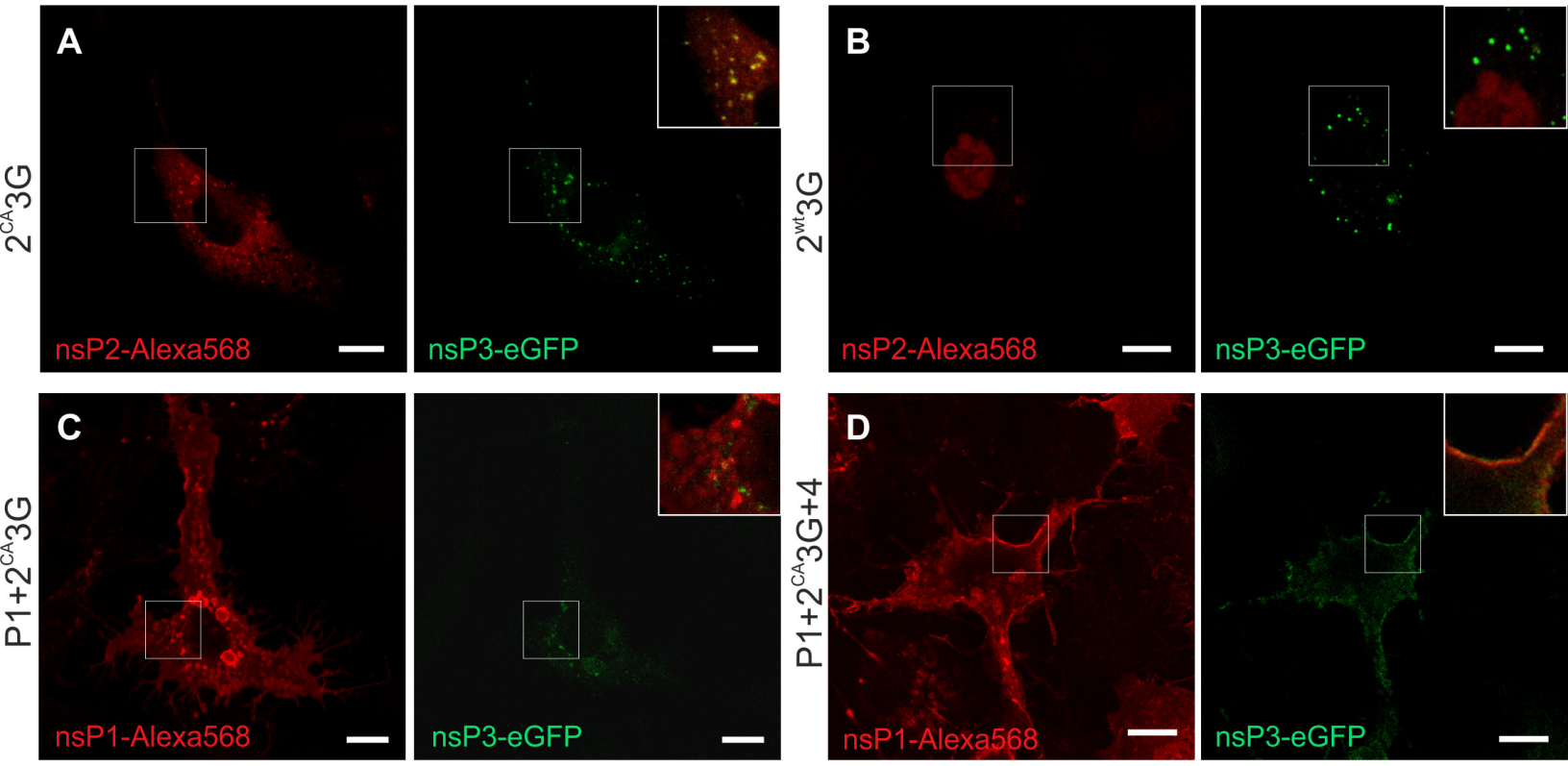
A
B
C
D
2CA3G
2wt3G
P1+2CA3G
P1+2CA3G+4
nsP2-Alexa568
nsP3-eGFP
nsP1-Alexa568
nsP3-eGFP
nsP2-Alexa568
nsP3-eGFP
nsP1-Alexa568
nsP3-eGFP

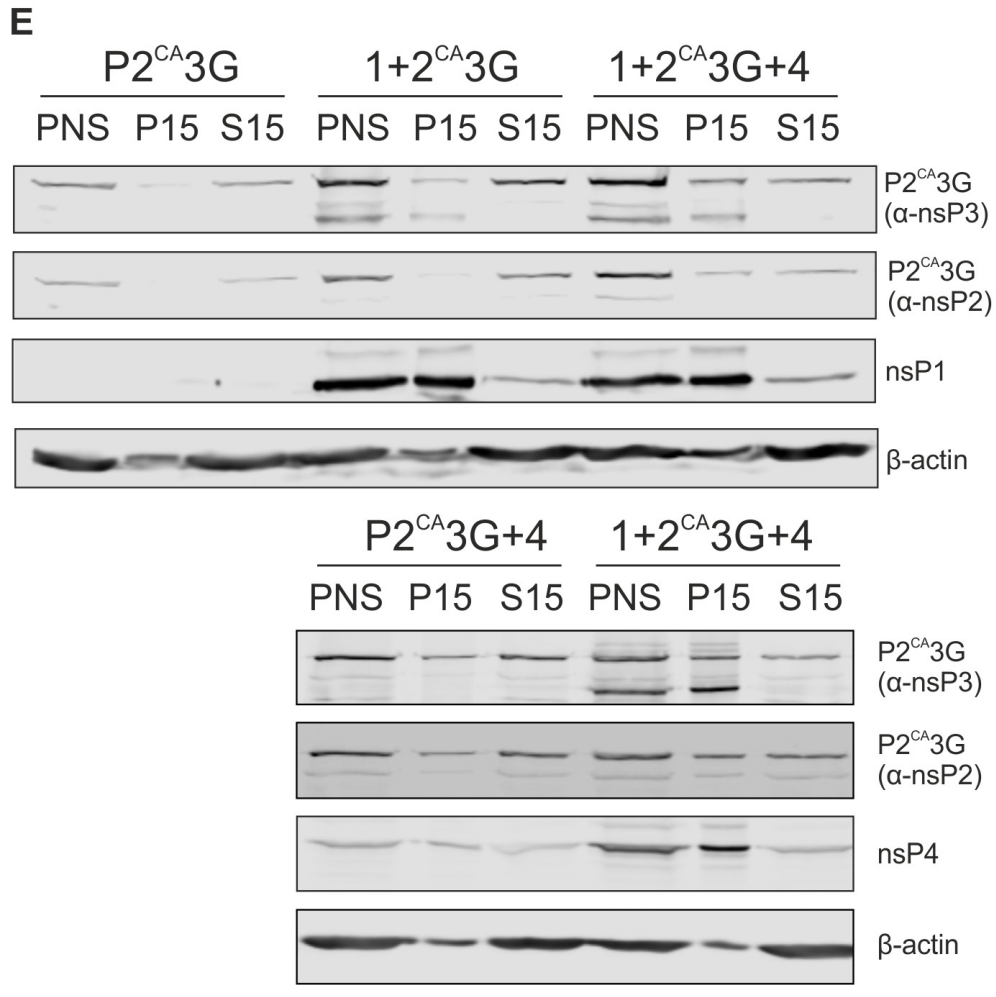
E
P2CA3G
1+2CA3G
1+2CA3G+4
PNS P15 S15 PNS P15 S15 PNS P15 S15
P2CA3G (α-nsP3)
P2CA3G (α-nsP2)
nsP1
β-actin
P2CA3G+4
1+2CA3G+4
PNS P15 S15 PNS P15 S15
P2CA3G (α-nsP3)
P2CA3G (α-nsP2)
nsP4
β-actin

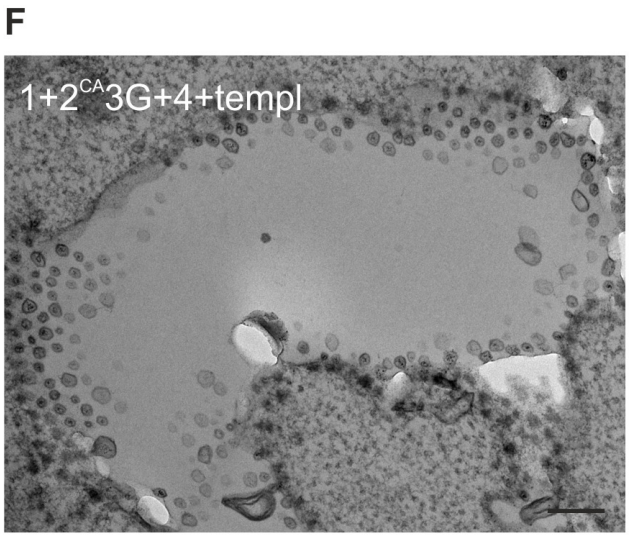
F
1+2CA3G+4+templ

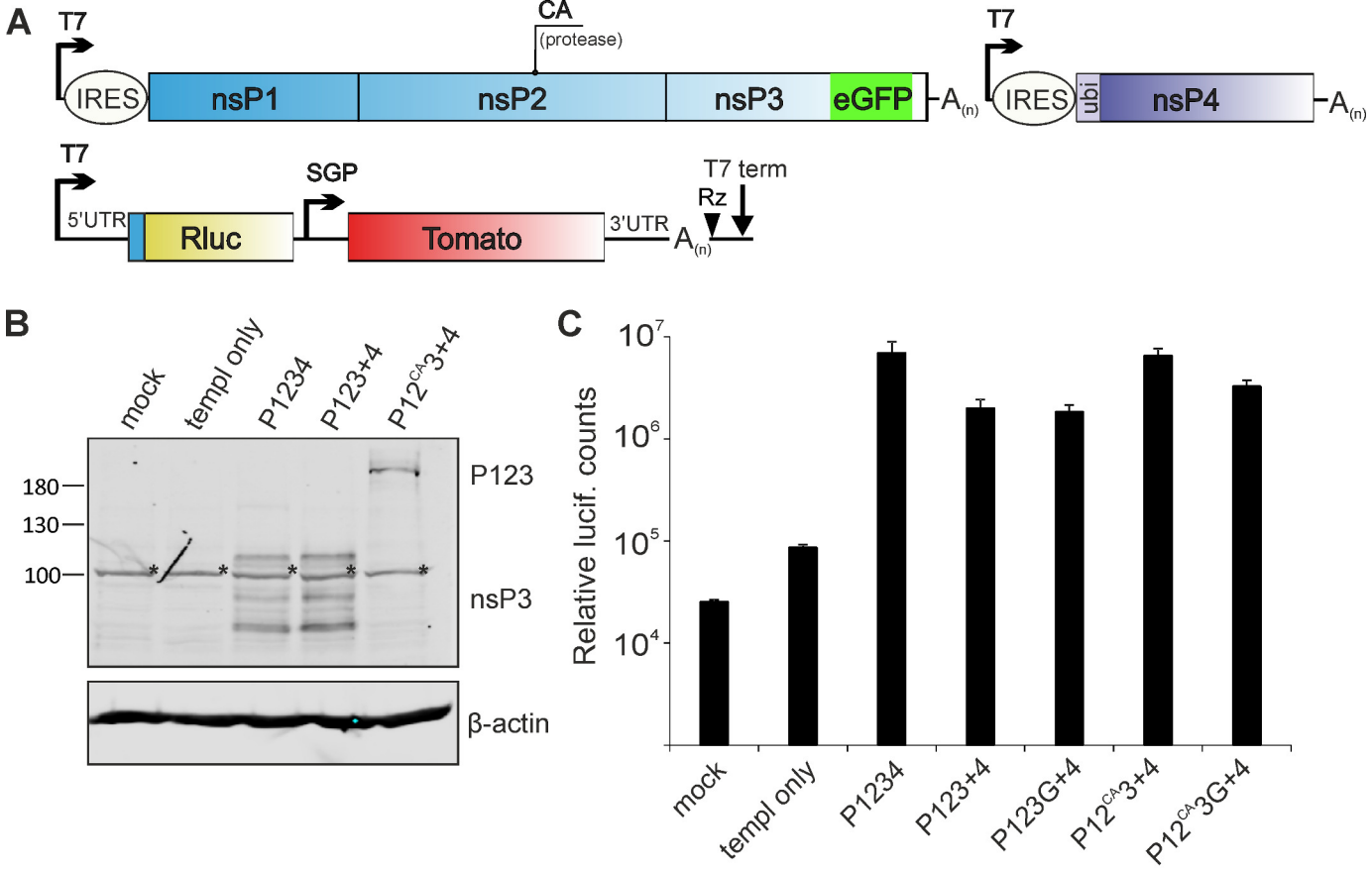
A
T7
IRES
nsP1
nsP2
CA
(protease)
nsP3
eGFP
A(n)
T7
IRES
ubi
nsP4
A(n)
T7
5'UTR
Rluc
SGP
Tomato
3'UTR
A(n)
T7 term
Rz
B
mock
templ only
P1234
P123+4
P12CA3+4
180
130
100
P123
nsP3
β-actin
C
Relative lucif. counts
10^7
10^6
10^5
10^4
mock
templ only
P1234
P123+4
P123G+4
P12CA3+4
P12CA3G+4
D
i
P12CA3G+4
ii
P123G+4
iii
P12CA3G+4+templ
E
P12CA3G+4
nsP2-Alexa568
nsP3-eGFP
merge
P123G+4
nsP2-Alexa568
nsP3-eGFP
merge